Carbohydrate Polymers 92 (2013) 23–32

Contents lists available at SciVerse ScienceDirect

Carbohydrate Polymers

journal homepage: www.elsevier.com/locate/carbpol

Multiresponsive macroporous semi-IPN composite hydrogels based on native or anionically modified potato starch

Ecaterina Stela Dragan*, Diana Felicia Apopei

"Petru Poni" Institute of Macromolecular Chemistry, Aleea Grigore Ghica Voda 41 A, RO-700487 Iasi, Romania

ARTICLE INFO

Article history:
Received 30 May 2012
Received in revised form 22 August 2012
Accepted 23 August 2012
Available online 30 August 2012

Keywords:
Composites
Hydrogels
Interpenetrating network (IPN)
Macroporous polymers
Potato starch

ABSTRACT

Macroporous semi-interpenetrating polymer networks (semi-IPN) composite hydrogels were synthesized by cross-linking polymerization of acrylamide (AAm) with N,N'-methylenebisacrylamide (BAAm) in the presence of potato starch (PS) or an anionic polyelectrolyte derived from PS (PA), below the freezing point of the reaction solution (−18 °C). The composite cryogels have been further modified by the partial hydrolysis of the amide groups in poly(acrylamide) (PAAm) matrix, under alkaline conditions. The influence of the entrapped polymer on the properties of the composite gels, both before and after the hydrolysis, has been evaluated by the swelling kinetics, FT-IR spectroscopy, scanning electron microscopy, and external stimuli responsiveness. The potential of the anionic composite cryogels as intelligent hydrogels has been evaluated by the investigation of the deswelling/reswelling kinetics as a function of solvent nature, ionic strength, and environment pH. Cryogels with fast responsivity at variation of the external stimuli, which withstood repeated deswelling/reswelling cycles, have been obtained at a low cross-linker ratio (one mole BAAm for 80 moles of AAm) and a monomer concentration around 3 wt%.

1. Introduction

Considerable interest has been focused last years on the ionic macroporous hydrogels due to the numerous applications in controlled delivery of drugs and proteins and separation processes of small ionic species (Baggiani, Baravalle, Giovanolli, Anfossi, & Giraudi, 2010; Dragan, Cazacu, & Nistor, 2009; Hajizadeh, Kirsebom, Galaev, & Mattiasson, 2010; Liu et al., 2011; Tekin, Uzun, Şahin, Bektaş, & Denizli, 2011). For the preparation of such materials, some strategies have been widely used: cross-linking polymerization in the presence of a pore-forming agent (Wu, Hoffman, & Yager, 1992), porogen leaching (Pradny et al., 2003; Serizawa, Wakita, Kaneko, & Akashi, 2002), cross-linking in the presence of substances releasing porogen gases (Behravesh, Jo, Zygourakis, & Mikos, 2002; Kim & Park, 2004), lyophilization of the hydrogel swollen in water (Dragan et al., 2009; Kang, Tabata, & Ikada, 1999), and cryogelation (Burova et al., 2011; Kirsebom, Topggard, Galaev, & Yu Mattiasson, 2010; Lozinsky, Plieva, Galaev, & Mattiasson, 2001; Orakdogen, Karacan, & Okay, 2011; Ozmen, Dinu, Dragan, & Okay, 2007; Savina et al., 2011; Zhao, Sun, Lin, & Zhou, 2010; Zhao, Sun, Wu, & Lin, 2011). By cryogelation, the cross-linking polymerization reactions are conducted below the freezing point of the reaction solutions, when the most part of the solvent (water, in the case of hydrogels) forms crystals, the bound water and the soluble substances (monomers, initiator, polymers) being concentrated in a non-frozen liquid microphase, where the gel is formed. Starting with Lozinsky et al. (Burova et al., 2011; Lozinsky et al., 2001), numerous research groups such as Galaev et al. (Kirsebom et al., 2010; Savina, Mattiasson, & Galaev, 2005; Savina et al., 2011), Okay et al. (Bilici, Karayel, Demir, & Okay, 2010; Orakdogen et al., 2011; Ozmen et al., 2007), Zhao et al. (Zhao et al., 2010, 2011) contributed to the fast development of this type of hydrogels. It is already established that, by their interconnected pore structure, cryogels allow the unhindered diffusion of solutes or even colloidal particles, making them very attractive in biomedicine and biotechnology including chromatographic materials, carriers for the immobilization of molecules and cells, matrices for cell separations, and cell culture (Baydemir et al., 2009; Burova et al., 2011; Dispinar, Van Camp, De Cock, De Geest, & Du Prez, 2012; Jain, Karande, & Kumar, 2011; Kathuria, Tripathi, Kar, & Kumar, 2009; Lozinsky et al., 2001; Savina et al., 2007). The mechanical properties and the diffusion of solutes in hydrogels can be further modulated by the preparation of multicomponent networks like semi-interpenetrating polymer networks (semi-IPN) or full-IPN. The biocompatibility and biodegradability of these multicomponent composite gels can be improved with biopolymers like polysaccharides, as components of the gel architecture (Baggiani et al., 2010; Jain et al., 2011; Kathuria et al., 2009; Liang, Liu, Huang, & Yam, 2009; Orakdogen et al., 2011; Van Vlierberghe, Dubruel, & Schacht, 2011).

Lately, much attention has been given to anionic multicomponent systems, these materials being appropriate for the

* Corresponding author.
E-mail address: sdragan@icmpp.ro (E.S. Dragan).

0144-8617/$ – see front matter © 2012 Elsevier Ltd. All rights reserved.
http://dx.doi.org/10.1016/j.carbpol.2012.08.082

sorption/delivery of cationic species. The anionic character can be achieved either using preformed polyanions or copolymers of anionic monomers (Jeon, Lei, & Kim, 2008; Kim & Shin, 2007; Kim, La Flamme, & Peppas, 2003; Murthy, Mohan, Sreeramulu, & Raju, 2006; Reis et al., 2008), or by partial hydrolysis of amide groups in poly(acrylamide) (PAAm) (Dragan, Perju, & Dinu, 2012; Li, Zhao, Teasdale, John, & Zhang, 2002; Zhao et al., 2010, 2011). Concerning the last strategy, there is a lack regarding the influence of the polymer trapped in a semi-IPN composite on the hydrolysis level of the matrix and on the properties of the composite gel after hydrolysis. In a previous work, it has been already shown that the semi-IPN hydrogels containing potato starch (PS) as entrapped polymer had a particular behavior in the sorption/desorption cycles of the model cationic dye, methylene blue, comparative with the semi-IPN hydrogels containing the polyanion (PA) resulted by the hydrolysis of polyacrylonitrile (PAN) chains grafted on potato starch (PS-*g*-PAN) as entrapped polymer (Dragan & Apopei, 2011). It was observed that the dye sorption capacity of the hydrogel containing PS monotonously increased with the increase of the regeneration steps, the eluent being aqueous solution of 0.1 M NaOH, while the composite containing PA has been less influenced by the regeneration steps. It was assumed that a partial hydrolysis of amide groups in the PAAm matrix occurred, more probable in the presence of PS than in the presence of PA. This different behavior prompted us to perform a systematic investigation of the gel properties, as a function of the polymer entrapped in the PAAm matrix, cross-linker ratio (molar ratio between N,N'-methylenebisacrylamide, BAAm, and AAm), and the polymer concentration in the gel, both before and after the hydrolysis. Moreover, macroporous composite gels will be prepared by cryopolymerization.

Therefore, the objectives of the paper were: (i) to prepare nonionic and anionic macroporous semi-IPN composite hydrogels with swelling properties tailored by the controlled hydrolysis of the semi-IPN cryogels based on PS or PA as polymers entrapped in a matrix of PAAm; (ii) to investigate the sensitivity of the novel anionic composite hydrogels at various external stimuli as a function of the nature of the entrapped polysaccharide and the post synthesis treatment. It is expected as the combination of PAAm and PS or its anionic derivative (PA) in the preparation of macroporous composite hydrogels to provide novel biocompatible composite materials with potential applications in biomedical fields. To evaluate the potential of the ionic composite cryogels for intelligent drug delivery systems, the deswelling/reswelling kinetics of the anionic cryogels as a function of solvent nature, ionic strength and environment pH have been tested.

2. Materials and methods

2.1. Materials

Acrylamide (Fluka), BAAm, ammonium persulfate (APS), N,N,N',N'-tetramethylethylenediamine (TEMED), all purchased from Sigma–Aldrich, were used as received. PS from Fluka, humidity content < 10%, was used as received. AN has been distilled at about 77 °C and kept at low temperature before use. Stock solutions of APS and TEMED were prepared by dissolving 0.2 g of APS and 0.625 mL of TEMED each in 25 mL of double distilled water. Stock solutions of BAAm were prepared by dissolving BAAm calculated for a certain cross-linker ratio in 25 mL of distilled water, at 30 °C, under magnetic stirring, and used for hydrogels synthesis after 24 h.

2.2. Preparation of PA from PS-g-PAN

For the preparation of PS-*g*-PAN copolymer, the redox initiation by Ce^{4+} ions has been adopted because it was demonstrated that the redox-initiated process of graft copolymerization onto the polysaccharide backbone generates free radicals on the polysaccharide backbone itself, a little space remaining for the homopolymerization if the monomer and initiator concentrations are lower than the critical concentrations, 2.0 M and 0.1 M, respectively (Karmakar, Rath, Sastry, & Singh, 1998; Qudsieh et al., 2008). In our experiments, the concentrations of monomer and Ce^{4+} have been kept lower than the critical concentrations. The details concerning the synthesis of PS-*g*-PAN with $Ce(SO_4)_2$ with a concentration of 0.02 M in 0.4 M H_2SO_4 have been previously presented (Apopei, Dinu, & Dragan, 2012; Dragan & Apopei, 2011). It was found that, in the synthesis conditions, PAN has been mainly grafted on the amylose and less on the amylopectin. Polyanion PA has been obtained by the alkaline hydrolysis of PS-*g*-PAN copolymer, the details concerning the preparation and characterization methods being given elsewhere (Dragan & Apopei, 2011). The content in carboxylate groups of the polyanion PA has been determined by polyelectrolyte titration with a standard solution of a strong oppositely charged polyelectrolyte, poly(diallyldimethylammonium chloride), with a concentration of 10^{-3} mol/L, using a particle charge detector PCD 03, Müteck GmbH, Germany (Mütek PCD-Titrator). The concentration of the negatively charged groups in the examined solution was calculated from the amount of standard solution needed to reach the zero value of the streaming potential. The content of poly(sodium acrylate) (NaPA) in PA thus determined was 0.788 g NaPA/g PA, which indicates a content of 7.44 meq COO^-/g PA.

2.3. Preparation and characterization of semi-IPN composite cryogels

Nonionic and anionic semi-IPN composite cryogels have been prepared by free radical cross-linking copolymerization of AAm and BAAm in the presence of gelatinized PS or hydrolyzed PS-*g*-PAN (PA) as entrapped polymer in aqueous medium, at −18 °C. Gelatinized PS was prepared by heating the starch dispersion (1 wt%) up to 80 °C, about 30 min, and used after cooling at room temperature. PA as aqueous solution with a concentration of 1 wt% has been prepared by stirring at room temperature, one day before using. The initial concentration of monomers (AAm + BAAm), C_0, has been either 3 or 5 wt% (Table 1). The redox initiator system consisted of APS and TEMED, the initiator concentrations being kept constant throughout the work.

The synthesis procedure used in the preparation of semi-IPN composite cryogels is briefly presented below, for X = 1:60. Typically, 0.4825 g AAm, 7 mL PS or PA solution (1 wt%), 1 mL BAAm and 1 mL TEMED stock solutions were first mixed in a graduated flask of 10 mL. The solution was cooled at 0 °C in ice-water bath, purged with nitrogen gas for 20 min and then, 1 mL of APS stock aqueous solution has been added, and the whole mixture has been further stirred about 20 s. Portions of this solution, each 1 mL, were transferred into syringes of 5 mm in diameter, in order to prepare gels in the shape of rods, and after that immersed in a thermostated bath at −18 °C, and the polymerization was conducted for one day. After polymerization, the gels were cut into pieces of about 10 mm in length. All gels were immersed in large volumes of Milli pore water to wash out any soluble polymers, unreacted monomers and the initiator, changing the washing water each 4 h. Cross-linked PAAm cryogel without PS or PA (PAAm.40.5, Table 1) has been prepared as reference, according to the protocol described above. Thereafter, the swollen gel samples have been stepwise dehydrated in water–acetone mixtures, the acetone content being 20% (3 h), 40% (3 h), 60% (3 h), 80% (3 h), 100% (12 h). In this way, the porosity of the gels in the dried state has been preserved.

Table 1
Samples code and feed composition of semi-IPN composite cryogels.

Sample	BAAm:AAm molar ratio	Polymer concentration, wt%	Entrapped polymer	
			Code	Content, wt%
PAAm40.5	1:40	5	–	–
PAAm/PS80.5	1:80	5	PS	12.28
PAAm/PS80.3	1:80	3	PS	12.28
PAAm/PS60.5	1:60	5	PS	12.28
PAAm/PS40.5	1:40	5	PS	12.28
PAAm/PA80.5	1:80	5	PA	12.28
PAAm/PA80.3	1:80	3	PA	12.28
PAAm/PA60.5	1:60	5	PA	12.28
PAAm/PA40.5	1:40	5	PA	12.28

2.4. Hydrolysis of PAAm under controlled conditions

Aqueous solution of 0.5 M NaOH has been used as hydrolysis agent in all experiments performed throughout the study because, from the previous investigations concerning the controlled hydrolysis of amide groups attached to the PAAm matrix, it was found that the hydrolysis level was increasing with the NaOH concentration up to 0.5 M, and remained almost constant irrespective of NaOH concentration up to 2 M (Dragan et al., 2012). After washing at neutral pH, the gels have been stepwise dehydrated in water–acetone mixtures as it has been shown above.

2.5. Characterization methods

2.5.1. FTIR analysis

The structure of semi-IPN composite cryogels, either before or after hydrolysis, has been investigated by FTIR spectroscopy. The dried samples have been first frozen in liquid nitrogen, and then broken in a mortar to get the samples as white powder. FTIR spectra were recorded with a Bruker Vertex FT-IR spectrometer, resolution 2 cm^{-1}, in the range of 4000–400 cm^{-1} by KBr pellet technique, the amount of the sample being about 5–8 mg in each pellet.

2.5.2. Morphological characterization

Surface morphology and internal structure of the dried composite gels were observed by an Environmental Scanning Electron Microscope (ESEM) type Quanta 200, operating at 20 kV with secondary electrons, in low vacuum mode. The cross-sections of the samples were performed using a sharp blade to revel the internal structures. The average diameter of pores was determined from the SEM photographs using the image analyzing program ACD Photo Editor v3.1, the sizes of 40 pores being averaged.

2.5.3. Swelling ratio and swelling kinetics

Swelling properties were studied using conventional gravimetric procedure (Dragan & Apopei, 2011; Murthy et al., 2006). The swelling behavior of dried hydrogels was determined by immersing the completely dried hydrogel samples in double-distilled water at 25 °C. Swollen gels were weighed by an electronic balance, at predetermined intervals, after wiping the excess surface liquid by filter paper. Based on the swelling experimental results, the swelling ratio, SR, equilibrium swelling ratio, SR_{eq}, and equilibrium water content, EWC, were calculated by Eqs. (1)–(3), respectively (Dragan & Apopei, 2011; Murthy et al., 2006):

$$SR = \frac{W_t - W_d}{W_d}, g \cdot g^{-1} \quad (1)$$

$$SR_{eq} = \frac{W_{eq} - W_d}{W_d}, g \cdot g^{-1} \quad (2)$$

$$EWC\ (\%) = \frac{W_{eq} - W_d}{W_{eq}} \times 100 \quad (3)$$

where W_d, W_t and W_{eq} are the weights of the sample in dried state, swollen state at time t and swollen at equilibrium, respectively. The measurements were performed in three replicates and average data were used for calculation of the swelling ratio.

3. Results and discussion

3.1. Preparation of semi-IPN composite cryogels

Semi-IPN composite cryogels as rods were prepared by the radical cross-linking copolymerization of AAm with BAAm in the presence of PS or PA, under the freezing point of the solvent (−18 °C). The ice crystals act as porogen during gelation, leading to a superporous structure by melting at the end of the gel preparation (Dinu, Perju, & Dragan, 2011; Kirsebom et al., 2010; Lozinsky et al., 2001; Orakdogen et al., 2011). The feed composition and the samples code of the composite gels are presented in Table 1. The general code of semi-IPN composite cryogels is PAAm followed by PS or PA for potato starch or polyanion used as entrapped polymer, respectively, and two numbers, separated by dots: the first one represents the mole number of AAm per one mole of BAAm and the second one represents the concentration of monomers.

It was expected as the gels properties like swelling kinetics and morphology to be influenced by the composition of the gels and also by the post-treatment consisting of the controlled hydrolysis of the composite gels under alkaline conditions. From the literature and our previous investigations it is known that the amide groups in PAAm easily hydrolyze in alkaline conditions generating COO^- groups (Ilavsky, Hrouz, Stejskal, & Bouchal, 1984). The alkaline hydrolysis of PAAm is self-retarded by the effect of the already formed neighboring carboxylate groups (COO^-), which reject the OH^- groups, the rate of hydrolysis decreasing with the increase of the hydrolysis degree (Dragan et al., 2012; Zhao et al., 2010, 2011). However, the influence of the entrapped polysaccharide in a matrix of PAAm on the hydrolysis level has been not pointed out yet. Therefore, in a preliminary investigation, the influence of the hydrolysis duration with NaOH 0.5 M on the equilibrium swelling ratio (SR_{eq}), and on the diameter of the PAAm/PS40.5 and PAAm/PA40.5 composite cryogels (D_{sw}), compared with PAAm40.5 taken as a reference, has been evaluated, the results being plotted in Fig. 1.

As can be observed from Fig. 1, the SR_{eq} values (Fig. 1A) and D_{sw} (Fig. 1B) abruptly increased after 2 h of hydrolysis, and remained almost constant up to 4 h of reaction, for all samples of cryogels. The SR_{eq} of PAAm40.5 cryogel, used as reference, increased from about 25 g/g, measured before hydrolysis, up to about 64 g/g, after 4 h of hydrolysis in 0.5 M aqueous solution of NaOH, at 25 °C (Fig. 1A). At the same time, the diameter of the cylinder in swollen state, D_{sw} (Fig. 1B), increased from about 5 mm, the diameter measured before the hydrolysis, up to about 7.3 mm, after the hydrolysis. As Fig. 1 shows, the SR_{eq} and D_{sw} values found for the semi-IPN composite gels have been strongly influenced by the nature of

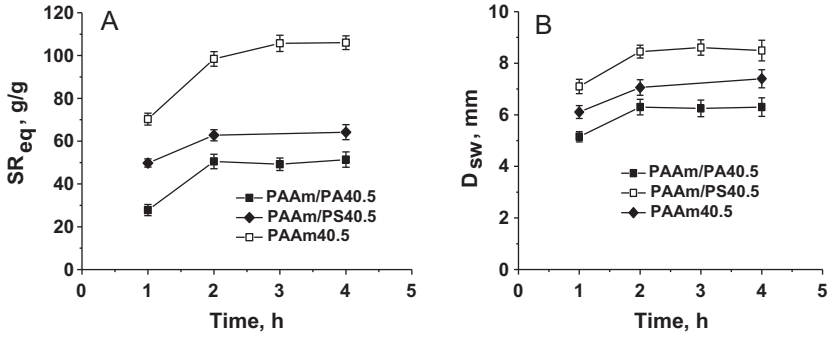

Fig. 1. Equilibrium swelling ratio, SR_{eq} (A) and swelling diameter, D_{sw} (B) of the composite gels as a function of the hydrolysis duration in aqueous solution of NaOH 0.5 M, at 25 °C.

the entrapped polymer, being significantly higher in the case of PAAm/PS40.5 compared with the reference PAAm40.5, and much higher than those of the gels containing PA (PAAm/PA40.5), irrespective of the hydrolysis duration. The hydrolysis duration of the cryogels investigated in the paper has been 3 h, because, according to Fig. 1, no significant changes of the SR_{eq} and D_{sw} occurred at longer durations.

3.2. Characterization of semi-IPN composite cryogels

3.2.1. FTIR analysis

The structural changes after the hydrolysis of PAAm/PS and PAAm/PA composite cryogels were supported by the FTIR spectroscopy. The FTIR spectra of the PAAm/PS40.5 and PAAm/PA40.5 cryogels, before and after the hydrolysis in NaOH 0.5 M, 3 h, are presented in Fig. 2.

It has been already shown that it is difficult to demonstrate the presence of polysaccharides (chitosan, for example) in a matrix of PAAm, because the characteristic bands of amide groups screen many of the characteristic bands of the entrapped polymers in semi-IPN composite gels (Dragan et al., 2012). Therefore, as Fig. 2 shows, in the spectra of the pristine semi-IPN composite cryogels, the characteristic bands of the PAAm matrix are the most visible. Thus, the peaks located at 1653 cm^{-1} and 1616 cm^{-1} (spectrum A) and at 1661 cm^{-1} and 1611 cm^{-1} (spectrum C), have been assigned to the stretching vibrations of the C═O bond in amide group, amide I band, and to the deformation vibrations of the N—H bond, amide II band, respectively; the peak at 1319 cm^{-1} (spectra A and C) has been assigned to the C—N stretching (amide-III band); the peaks located at 1120 cm^{-1}, in the spectrum of PAAm/PS40.5 (spectrum A) and at 1118 cm^{-1}, in the spectrum of PAAm/PA40.5 (spectrum C) have been assigned to the C—N stretching in secondary amide from BAAm in PAAm matrix. Even if in the FTIR spectrum of PA the characteristic peaks of the anhydroglucose ring (1155 cm^{-1}, 1081 cm^{-1}, and 1024 cm^{-1}), and for the COO^- groups (1553 cm^{-1}, assigned to stretching vibration of —COO^- groups, and 1404 cm^{-1} assigned to the symmetric stretching of C═O in —COO^- groups) have been clearly observed (Dragan & Apopei, 2011), they are not visible in the spectrum of PAAm/PA40.5 composite gel. Therefore, to support the strong influence of PAAm matrix on the characteristic bands of PA, the spectrum of a physical mixture PAAm:PA, 4:1 (wt/wt) (PAAm:PA ratio being lower than in semi-IPN cryogels, which, according to Table 1, is around 7:1) has been recorded (not included in Fig. 2). Only the band at 1032 cm^{-1}, assigned to the stretching vibration of the C—O bonds in anhydroglucose ring, has been more intense than in the PAAm/PA cryogels. The other characteristic bands of PA have been screened by those of PAAm.

However, the spectra of the composite cryogels, after the controlled hydrolysis (spectra B and D), clearly support the partial hydrolysis of amide groups by the peaks located at 1560 cm^{-1}, and 1401 cm^{-1} (spectrum B), and at 1556 cm^{-1}, and 1404 cm^{-1} (spectrum D). The new peaks assigned to C═O in carboxylic acids, at 1560 cm^{-1}, spectrum C, and at 1556 cm^{-1}, spectrum D, and to COO^- groups, at 1401 cm^{-1}, spectrum B, and at 1404 cm^{-1}, spectrum D,

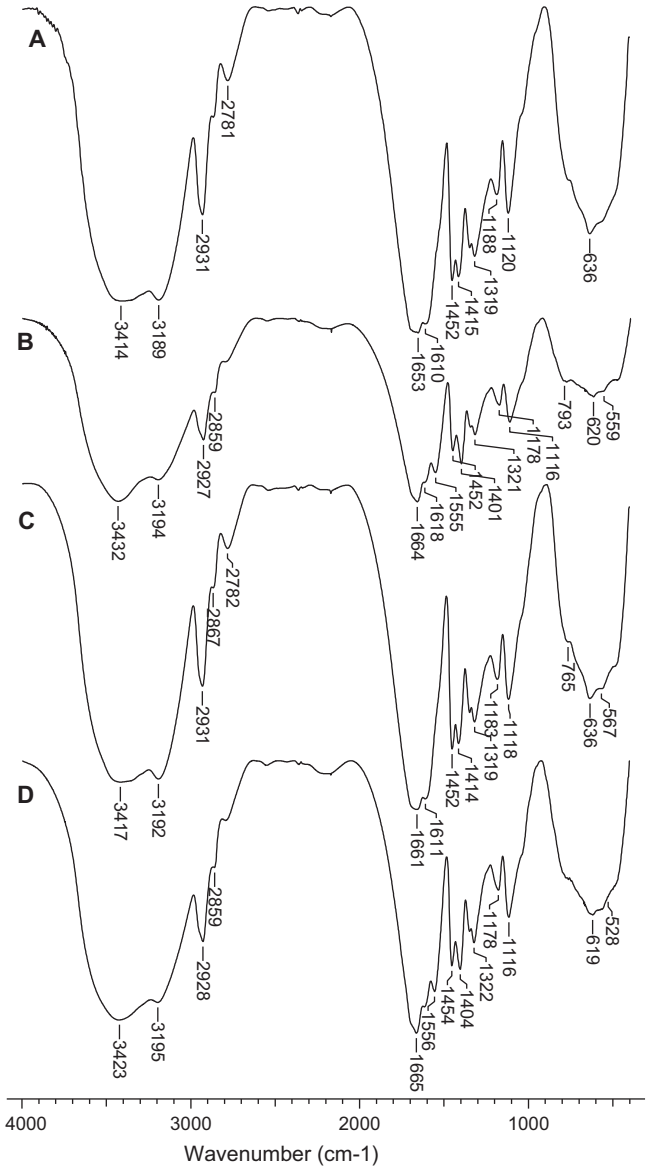

Fig. 2. FTIR spectra of PAAm/PS40.5 (A and B) and PAAm/PA40.5 (C and D) before (A and C) and after the hydrolysis in NaOH 0.5 M, 3 h (B and D).

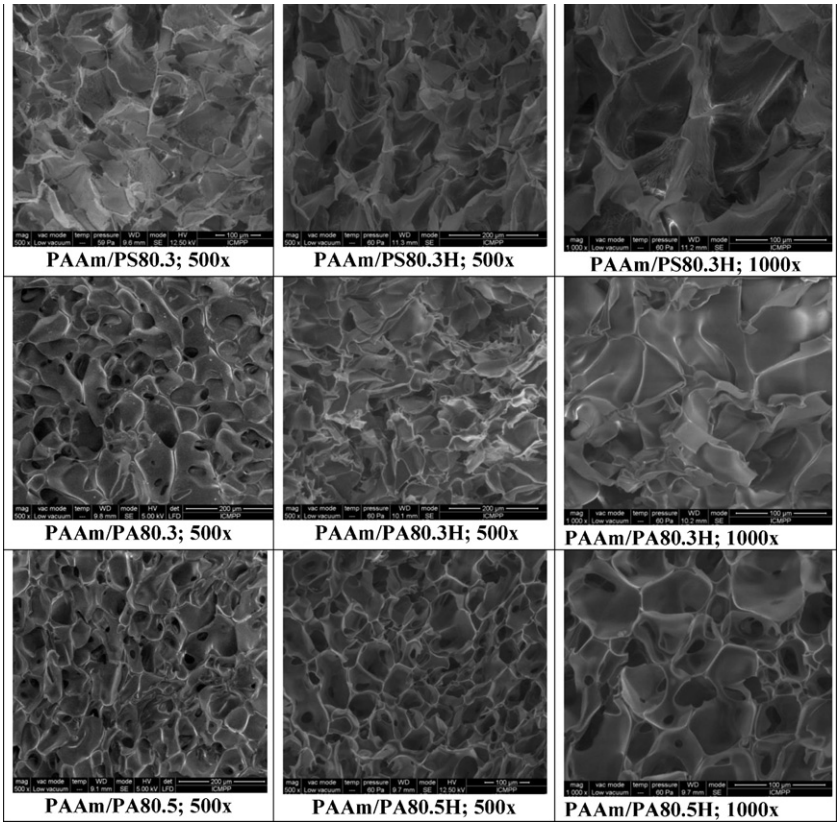

Fig. 3. SEM images of PAAm/PS80.3, PAAm/PA80.3, and PAAm/PA80.5 composite cryogels, before (left column) and after (middle and right columns) hydrolysis.

which were not observed in the initial cryogels, support the hydrolysis of part of the amide groups. The peak at 1664 cm^{-1}, assigned to the stretching vibration of C=O in amide groups, supports the presence of non-hydrolyzed acrylamide units.

3.2.2. Morphological analysis

Scanning electron microscopy, SEM, has been used to investigate the surface morphology and internal structure of the dried cryogel samples. The images presented in Fig. 3 illustrate the influence of the polymer entrapped and of the initial monomer concentration, at a cross-linker ratio of 1/80, on the internal morphology and pore sizes, before and after the gel hydrolysis. The gel morphology in the swollen state was preserved by the stepwise dehydration of the gels in water–acetone mixtures.

As Fig. 3 shows, the internal morphology (the size and geometry of pores) of the samples prepared with a monomer concentration of 3 wt% is strongly influenced by the entrapped polymer structure, the average pore size being 67 μm for PAAm/PS80.3 (first line) and 62 μm for PAAm/PA80.3 (middle line). As can be seen, the morphology of selected gels changed in a different way after hydrolysis. Interconnected macropores with sizes in the range 80–82 μm can be observed in the SEM image of PAAm/PS80.3H, while a smaller influence of hydrolysis is evident in the case of the sample PAAm/PA80.3H, pore sizes decreasing to around 53 μm (the difference is more visible at a magnification of 1000×). The larger pores found in the case of PAAm/PS80.3H than in the case of PAAm/PA80.3H are attributed to the higher swelling degree of PAAm/PS80.3H, caused by a higher density of the anionic groups ($-COO^-$) generated by a higher level of hydrolysis of PAAm matrix of the first gel (supported also by Fig. 1). We assumed that the level of hydrolysis has been diminished by the presence of the anionic polyelectrolyte (PA) as entrapped polymer, which contributed to the decrease of the concentration of OH^- ions in the interior of the gel by the presence of $-COO^-$ groups. The hydrolysis of the PAAm matrix at a different level is also supported by the comparison of the pore walls of the gels after hydrolysis, these being thicker for PAAm/PS80.3H than for PAAm/PA80.3H. Moreover, polyelectrolyte PA could be better entangled in the matrix, while part of amylose in PS could be removed during the hydrolysis step, thus acting as a porogen, leading to the enlarge of the pore sizes.

The increase of the monomer concentration has a definite influence on the morphology of the gels based on PA (sample PAAm/PA80.5, the last line, compared with sample PAAm/PA80.3, the middle line). Polyhedral interconnected pores can be seen in the SEM images of PAAm/PA80.3 and PAAm/PA80.5 before hydrolysis, the pore size decreasing with the increase of the monomer concentration (58 μm for PAAm/PA80.5 compared with 62 μm for PAAm/PA80.3). The pore size and geometry of the pores have been influenced by the controlled hydrolysis, the influence being more evident at a lower concentration of monomers (PAAm/PA80.3H compared with PAAm/PA80.5H). The higher decrease of the pore size after hydrolysis in the case of the gel with lower concentration of monomers (3%) (PAAm/PA80.3H) is explained by the fact that this gel was weaker than the gel having 5% of monomers (PAAm/PA80.5H).

SEM morphological cross-section patterns of the semi-IPN composite cryogels having cross-linker ratio of 1:60, and monomer concentration of 5 wt%, but different by the entrapped polymer nature are presented in Fig. 4, both before (up) and after (down) the controlled hydrolysis.

The cross-sectional features of the hydrogel networks are depending on the polymer nature, as it has been already observed above at the cross-linker ratio of 1/80 (Fig. 3). Thus, the PAAm/PA60.5 composite cryogel has a sponge like structure similar with that presented in Fig. 3 for PAAm/PA80.5, with interconnected pores with sizes of around 60 μm. On the other hand,

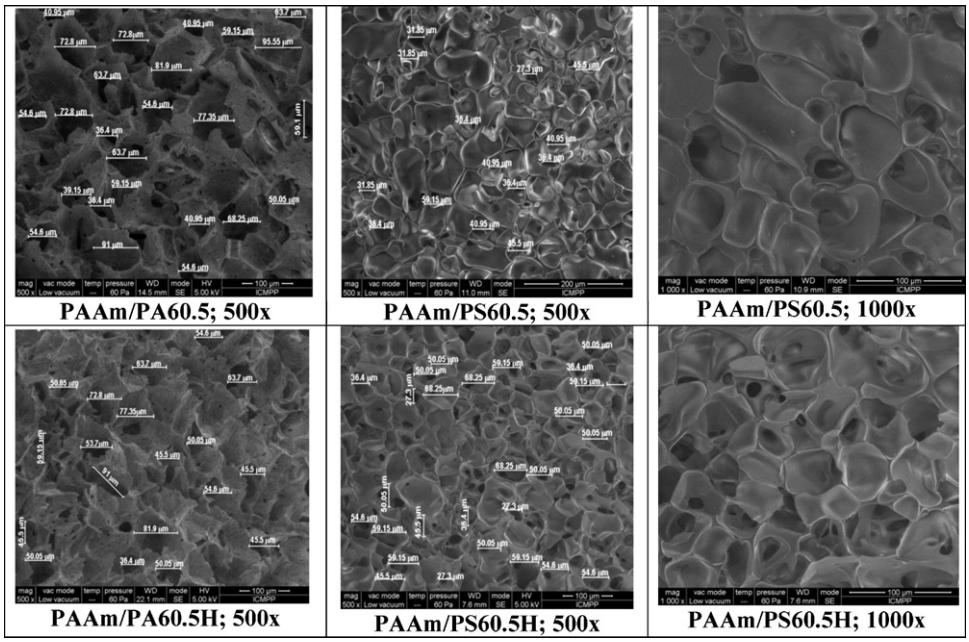

Fig. 4. SEM images of PAAm/PS.60.5 and PAAm/PA.60.5 composite cryogels, before (up) and after (down) hydrolysis.

the PAAm/PS60.5 composite cryogel reveals a more compact morphology, the pore sizes being much smaller than those found in PAAm/PA60.5 cryogel, around 39 μm. The down images in Fig. 4 show the morphologies of the same semi-IPN composite cryogels, after hydrolysis. A strong influence of the polymer entrapped nature on the changes of the gel morphology after hydrolysis can be observed, the main difference consisting of the size and geometry of pores. Thus, the pores size in PAAm/PA60.5 has been less influenced by the hydrolysis, the average size of pores being around 57.5 μm (SEM image, down, left), while the size of pores dramatically increased after the hydrolysis of PAAm/PS60.5 (clear observed at a magnification of 1000×, SEM image, down, right), the average size being around 50 μm. These differences also support the higher level of hydrolysis of the gel having gelatinized PS entrapped than of the gels based on the polyelectrolyte PA.

By comparison the pore sizes of the gels PAAm/PA80.5 (Fig. 3) and PAAm/PA60.5 (Fig. 4), which have the same entrapped polymer and initial monomer concentration, the influence of the cross-linker ratio can be seen, the pore sizes being higher when $X = 1/80$ than when $X = 1/60$, both before and after the hydrolysis.

3.2.3. Swelling ratio and swelling kinetics

Swelling ratio, SR (calculated with Eq. (1)), as a function of contact time for the PAAm/PS cryogels (A), and PAAm/PA cryogels (B) with two cross-linker ratios is presented in Fig. 5. The swelling kinetics of the PAAm/PS60.5 and PAAm/PA60.5 cryogels, after the hydrolysis, have been also included in Fig. 5.

As Fig. 5 shows, both types of semi-IPN cryogels present a superfast swelling, which is characteristic for the cryogels, the main difference consisting of the time necessary to reach the equilibrium swelling, this being around 30 s in the case of PAAm/PS and 15 s in the case of PAAm/PA, at the same cross-linker ratio. However, the influence of the entrapped polymer nature on the swelling behavior after hydrolysis of the gels with a cross-linker ratio of 1:60 is obvious in Fig. 5, the SR values of the PAAm/PS60.5H being much higher than those of PAAm/PA60.5H, i.e., 140 g/g compared with 50 g/g, respectively. These results suggest that the presence of PA, bearing a high number of negative charges, diminished the level of hydrolysis of the amide groups attached to the matrix. On the other hand, the presence of PS enhanced the hydrolysis level leading to much higher values of SR than those found when PA has been entrapped in the composite cryogels.

Equilibrium swelling ratio, SR_{eq}, and the equilibrium water content, EWC, calculated with Eqs. (2) and (3), respectively, as a function of pH, for semi-IPN composite cryogels, before and after the hydrolysis, have been plotted in Fig. 6. As can be seen, the SR_{eq} values of PAAm/PS60.5 composite gel, before the hydrolysis, are influenced by pH at a low level, increasing from about 30 g/g up to 35 g/g when pH increased from 1 to 11. At the same time, the SR_{eq} values of PAAm/PA60.5 gel increased from about 32 g/g up to 44 g/g, when pH increased from 1 to 10, respectively, increasing more for

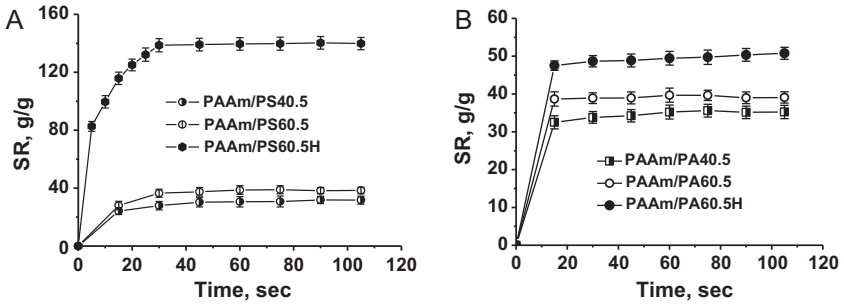

Fig. 5. Swelling ratio, SR, as a function of time for PAAm/PS cryogels (A) and PAAm/PA cryogels (B).

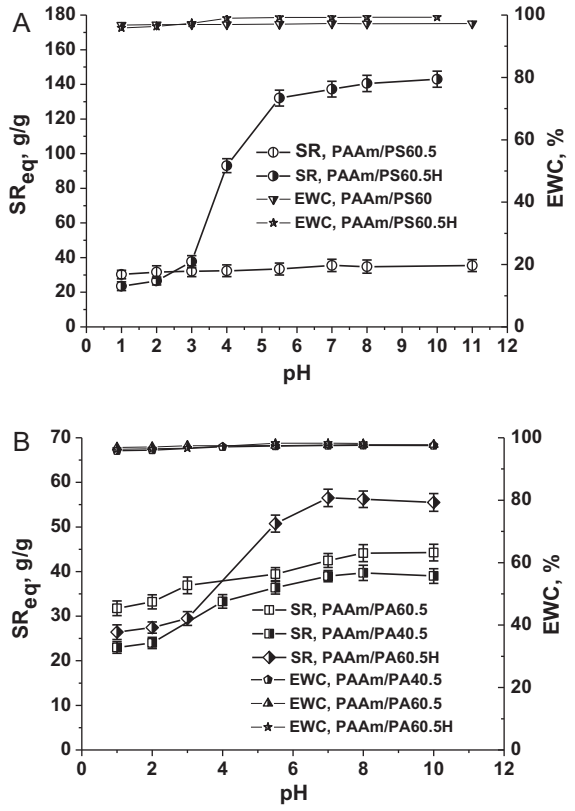

Fig. 6. Equilibrium swelling ratio, SR_{eq}, and equilibrium water content, EWC, as a function of pH for PAAm/PS cryogels (A) and PAAm/PA cryogels (B).

$X = 1/60$ than for $X = 1/40$. The increase of the SR_{eq} with the decrease of the cross-linker concentration is a characteristic of all hydrogels (Dragan et al., 2012; Murali Mohan, Joseph, & Geckeler, 2007).

The SR_{eq} values higher for PAAm/PA60.5 than for PAAm/PS60.5 before hydrolysis are explained by the higher hydrophilicity of the anionic polyelectrolyte, PA, than that of the pristine PS. On the other hand, after the controlled hydrolysis, the pH sensitivity of the composite gels, having the same cross-linker ratio, but different by the entrapped polymer, has been dramatically changed. As Fig. 6A shows, the SR_{eq} of PAAm/PS60.5H increased from 23 g/g, found at pH 1, up to about 143 g/g, found at pH 10, while the SR_{eq} of PAAm/PA60.5H (Fig. 6B) increased from 26.4 g/g, found at pH 1, up to 55.5 g/g, found at pH 10. After hydrolysis, the values of SR_{eq} at pH < 3, have been lower than those found before hydrolysis, more for PAAm/PA60.5H than for PAAm/PS60.5H. This difference can be attributed to the less hydrophilicity of COOH groups at pH lower than the pK_a of poly(acrylic acid) (4.8). The gel dramatically swells at pH > 3 due to the electrostatic repulsion between the numerous $-COO^-$ groups generated by the partial hydrolysis of amide groups. The strong difference between the swelling behavior of PAAm/PS60.5H and PAAm/PA60.5H as a function of pH is attributed to the nature of the entrapped polymer. It seems that PA had a negative impact on the hydrolysis of amide groups, because the high density of COO^- groups attached on the chain rejected the OH^- ions from the vicinity of the amide groups, keeping the hydrolysis at a lower level.

As Fig. 6 shows, the values of *EWC* slightly increased from about 96% to 98% with the increase of pH from 1 to 5.5, and remained almost constant up to pH 10, irrespective of the gel composition. The high values of *EWC* have been attributed to the low initial concentration of monomers (AAm + BAAm) (5%, for these samples). A small variation of the *EWC* with the content of cross-linker has been reported in the literature for other hydrogels at a constant concentration of monomers (Murali Mohan et al., 2007).

3.2.4. Deswelling/reswelling kinetics as a function of external stimuli

The rapid response rate to the external stimuli of the smart hydrogels is the most essential function for their applications, and therefore various methods have been used to increase the response kinetics (Bilici et al., 2010; Dogu & Okay, 2006; Zhang, Yang, Chung, & Ma, 2001; Zhao, Sun, Ling, & Zhou, 2009). It has been reported that the macroporous hydrogels have shown a much more rapid swelling–deswelling rate than the conventional hydrogels (Dogu & Okay, 2006; Zhang et al., 2001; Zhao et al., 2009). The deswelling/reswelling kinetics of some macroporous composite

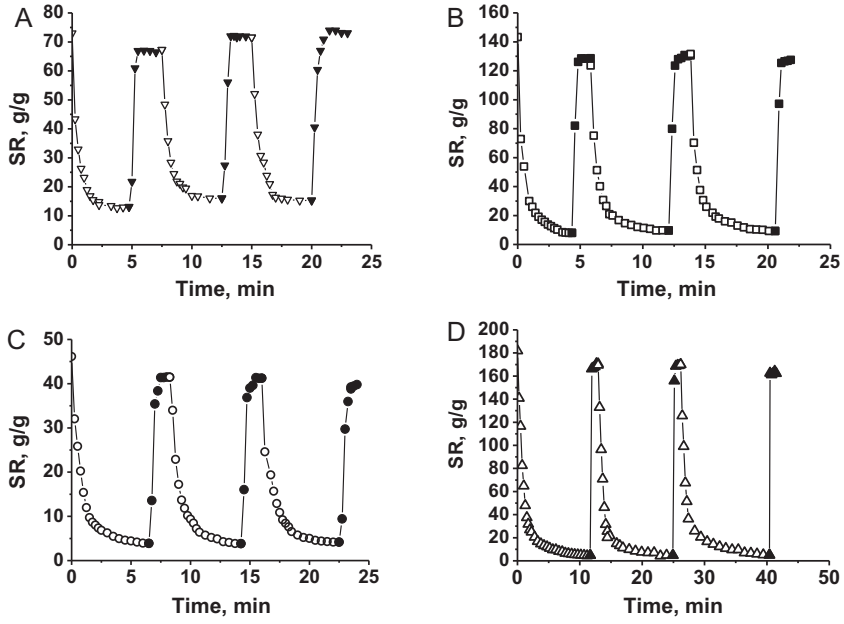

Fig. 7. Deswelling (empty symbols)–reswelling (full symbols) kinetics of semi-IPN anionic composite cryogels in ethanol/water: (A) PAAm/PS80.3H (down triangle); (B) PAAm/PA80.3H (square); (C) PAAm/PA80.5 (circle); (D) PAAm/PA80.5H (up triangle).

cryogels having the same cross-linker ratio, $X = 1/80$, but different by the nature of the entrapped polymer and by the initial concentration of monomers, in a good solvent/poor solvent pair, are presented in Fig. 7.

The gels have been first swollen at equilibrium in water, and thereafter the swollen gels have been immersed in ethanol as poor solvent. The deswelling process has been monitored by the gravimetric method, the weight of the gel being measured as a function of the deswelling time, until the collapsed gel reached the equilibrium. The reswelling/deswelling cycle in water/ethanol has been repeated up to three cycles. As Fig. 7 shows, the swelling response rate of the collapsed cryogels is super-fast for all gels, but the deswelling response rate of the same gel from its equilibrium swollen state is depending on the gel structure. As Fig. 7A shows, the PAAm/PS80.3H composite gel attained its equilibrium collapsed state within about 5 min, whereas the reswelling at the same initial SR required few seconds. A similar behavior has been found in the case of PAAm/PA80.3H (Fig. 7B), the time required to attain the equilibrium collapsed state being around 7 min. The longer time necessary for dehydration in the last case could be attributed to the presence of polyelectrolyte PA, which has a higher hydrophilicity than PS. The influence of the post-hydrolysis on the deswelling response rate of the gels can be observed in Fig. 7C and D, where the deswelling/reswelling cycles for the composite gel PAAm/PA80.5 before (Fig. 7C) and after (Fig. 7D) hydrolysis are presented. As can be seen, the PAAm/PA80.5 cryogel attains its equilibrium collapsed state in 6–7 min, its swelling rate is fast (about 30 s), and furthermore it shows the same values of the SR_{eq} in swollen state, at the end of the third cycle. After hydrolysis, the time required to attain the equilibrium collapsed state increased up to 12 min, probably due to the difficulties in the dehydration of the gel having a higher density of anionic sites.

The influence of the monomer concentration on the deswelling/reswelling kinetics is illustrated in Fig. 7B and D where the gels PAAm/PA80.3H and PAAm/PA80.5H have been compared. As can be observed, there is a strong difference between the composite cryogels concerning their response at the solvent quality as a function of the initial monomer concentration. Thus, while the PAAm/PA80.3H gel needs 20 min for three deswelling/reswelling cycles, the PAAm/PA80.5H sample needs 40 min, for the same number of cycles, i.e., the lower concentration of monomers the faster the deswelling step (water molecules are easier replaced by the poor solvent molecules).

The ionic character of the semi-IPN composite cryogels, with polyanion entrapped in the PAAm matrix, recommends them as materials responsive to electrolytes. The influence of the ionic strength on the SR_{eq} values of the gel PAAm/PA80.5, both before and after hydrolysis, has been followed first. As Fig. 8A shows, the swelling of PAAm/PA80.5 in aqueous solutions of NaCl, with concentrations in the range 0.1–1 M, showed a small but monotonous decrease of the SR_{eq} values with the increase of NaCl concentration up to 0.5 M. The influence of NaCl concentration on the SR_{eq} values of the PAAm/PA80.5.H showed a much stronger influence of the NaCl concentration, an abrupt decrease of the SR_{eq} values with the increase of NaCl concentration being observed (Fig. 8A). The difference is explained by the higher density of anionic centers in the gel after hydrolysis, leading thus to a higher sensitivity of the gel at the changes of the ionic strength in the environment.

As Fig. 8A shows, the critical concentration of NaCl asked by the cryogel PAAm/PA80.5H to attain the equilibrium collapsed sate is 1 M, SR_{eq} values being the same at concentrations up to 2 M. Therefore, for the study of the deswelling/reswelling kinetics in response at changing of the ionic strength, two samples of hydrolyzed cryogels different by the polymer content have been selected, PAAm/PA80.5H (Fig. 8B) and PAAm/PA80.3H (Fig. 8C), one cycle consisting of 1 M NaCl/pure water.

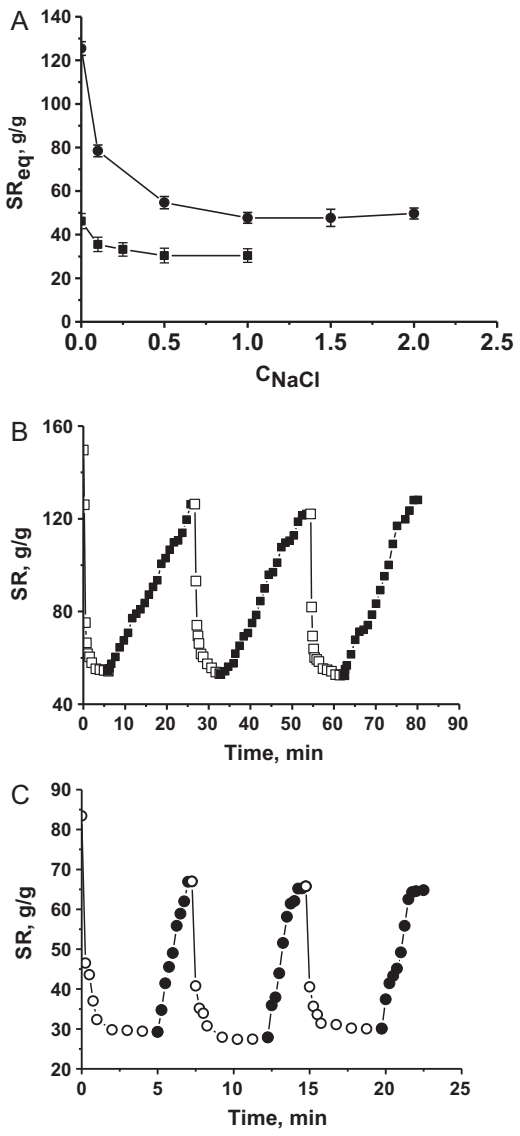

Fig. 8. (A) SR_{eq} as a function of NaCl concentration for PAAm/PA80.5 cryogel (full square) and PAAm/PA80.5H cryogel (full circle); (B) deswelling (empty symbols)/reswelling (full symbols) kinetics of PAAm/PA80.5H cryogel in 1 M NaCl aqueous solution/pure water; (C) deswelling (empty symbols)/reswelling (full symbols) kinetics of PAAm/PA80.3H cryogel in 1 M NaCl aqueous solution/pure water.

As can be observed in Fig. 8B, the semi-IPN PAAm/PA80.5H gel attained the equilibrium reswelling in 20 min, this process being slower than the deswelling step, which needed only 5 min. This behavior can be explained by the slow diffusion of the electrolyte ions from the collapsed gel, when the gel is immersed in pure water. On the other hand, the gel formed at $C_0 = 3\%$ (PAAm/PA80.3H) attained both its equilibrium collapsed state and the equilibrium swollen state in 2 min (Fig. 8C). The slower response rate of PAAm/PA80.5H composite gel at reswelling in pure water compared with PAAm/PA80.3H gel, having a lower concentration in polymer, can be attributed to the higher density of polymer–polymer contacts caused by the excess of Na^+ counterions. The time required to attain the equilibrium collapsed state has been also influenced by the monomer concentration, being longer at a higher concentration of monomer (5 min for PAAm/PA80.5H, and 2 min for PAAm/PA80.3H). This difference may be related to the cohesional forces between the hydrated chains of the ionic gel, which increase with the increase of the monomer concentration. The decrease of the equilibration time with the decrease

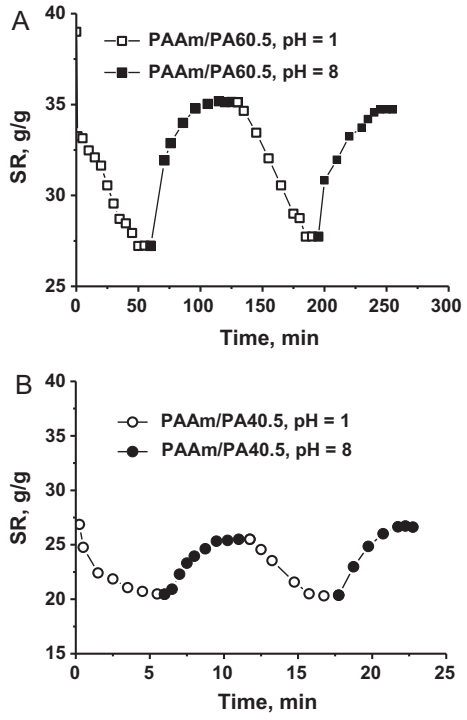

Fig. 9. Deswelling (empty symbols)–reswelling (full symbols) kinetics of PAAm/PA60.5 cryogel (A) and PAAm/PA40.5 cryogel (B) at pH 1 and pH 8, respectively.

of the monomer concentration has been already reported for the deswelling/reswelling cycles of the cryogels based on poly(acrylic acid) in methanol/water as good solvent/poor solvent (Bilici et al., 2010).

The presence of COO^- groups in the gels prepared with PA as entrapped polymer or the hydrolyzed gels make them sensitive to the pH changes (as it has been shown in Fig. 6). To evaluate the deswelling/reswelling kinetics of the PAAm/PA composite gels, the gels have been first swollen in water at pH 8 and after that their response at the alternation of pH between 1 and 8 has been followed as a function of time (Fig. 9). As can be seen in Fig. 9A, the response at pH changes of the PAAm/PA60.5 cryogel was relatively slow, the equilibrium collapsed state and the equilibrium swollen state being attained in the same interval of time, about 50 min.

On the other hand, as Fig. 9B shows, the response at pH changes of the gel having a higher cross-linker ratio (PAAm/PA40.5, $X = 1:40$) has been 10 times faster, both equilibrium collapsed state and the equilibrium swollen state being attained in about 5 min. This difference indicates that the increase of the cross-linker ratio would increase the response of the gel at the variation of pH.

4. Conclusions

Herein we have described the preparation of some novel macroporous semi-IPN composite cryogels having native PS or anionically modified PS (PA) entrapped in a matrix of PAAm. Examination of the SEM images showed that the morphology of semi-IPN composite gels has been strongly influenced by the entrapped polysaccharide and by the post treatment of the gels by hydrolysis. Thus, before hydrolysis the PAAm/PA60.5 composite cryogel had a sponge like structure, with interconnected pores, macropores with sizes of about 60 μm, while the PAAm/PS60.5 composite cryogel revealed small pores, the pore sizes being around 39 μm. The pores size in PAAm/PA60.5 has been less influenced by the hydrolysis, while the pore size increased after the hydrolysis of PAAm/PS60.5 up to 50 μm. All semi-IPN cryogels present a super-fast swelling, the main difference consisting of the time necessary to attain the equilibrium swelling, this being around 30 s in the case of PAAm/PS gels and 15 s in the case of PAAm/PA gels, at the same cross-linker ratio. It was observed that when the cross-linker ratio was 1:60 or higher, the presence of anionically modified PS, bearing a high number of negative charges, diminished the level of hydrolysis of the amide groups attached to the matrix, while the presence of native PS enhanced the hydrolysis level. The anionic character of the gels having PA as entrapped polymer before the hydrolysis and after that, and of the composite cryogels having gelatinized PS entrapped in the PAAm matrix, only after hydrolysis, has been demonstrated by the increase of SR_{eq} values at pH > 3. The study of the deswelling/reswelling kinetics of the composite gels, having a low cross-linker ratio (1:80), in ethanol/water and 1 M NaCl/water showed a higher responsivity of the anionic gels with $C_0 = 3\%$ than of those with $C_0 = 5\%$, which support the potential of these gels as "smart" hydrogels.

Acknowledgment

This work was supported by CNCSIS-UEFISCSU by the project PN-II-ID-PCE-2011-3-0300.

References

Apopei, D. F., Dinu, M. V., & Dragan, E. S. (2012). Graft copolymerization of acrylonitrile onto potatoes starch by ceric ion. *Digest Journal of Nanomaterials and Biostructures*, *7*, 707–716.

Baggiani, C., Baravalle, P., Giovanolli, C., Anfossi, L., & Giraudi, G. (2010). Molecularly imprinted polymer/cryogel composites for solid-phase extraction of bisphenol A from river water and wine. *Analytical and Bioanalytical Chemistry*, *397*, 815–822.

Baydemir, G., Bereli, N., Andac, M., Say, R., Galaev, I. Y., & Denizli, A. (2009). Bilirubin recognition via molecularly imprinted supermacroporous cryogels. *Colloids and Surfaces B: Biointerfaces*, *68*, 33–38.

Behravesh, E., Jo, S., Zygourakis, K., & Mikos, A. G. S. (2002). Synthesis of in situ cross-linkable macroporous biodegradable poly(propylene fumarate-co-ethylene glycol) hydrogels. *Biomacromolecules*, *3*, 374–381.

Bilici, C., Karayel, S., Demir, T. T., & Okay, O. (2010). Self-oscillating pH-responsive cryogels as possible candidates of soft materials for generating mechanical energy. *Journal of Applied Polymer Science*, *118*, 2981–2988.

Burova, T. V., Grinberg, N. V., Kalinina, E. V., Ivanov, R. V., Lozinsky, V. I., Lorenzo, C. A., et al. (2011). Thermoresponsive copolymer cryogel possessing molecular memory: Synthesis, energetics of collapse and interaction with ligands. *Macromolecular Chemistry and Physics*, *212*, 72–80.

Dinu, M. V., Perju, M. M., & Dragan, E. S. (2011). Composite IPN ionic hydrogels based on polyacrylamide and dextran sulfate. *Reactive and Functional Polymers*, *71*, 881–890.

Dispinar, T., Van Camp, W., De Cock, L. J., De Geest, B. G., & Du Prez, F. E. (2012). Redox-responsive degradable PEG cryogels as potential cell scaffolds in tissue engineering. *Macromolecular Bioscience*, *12*, 383–384.

Dogu, Y., & Okay, O. (2006). Swelling–deswelling kinetics of poly(N-isopropylacrylamide) hydrogels formed in PEG solutions. *Journal of Applied Polymer Science*, *99*, 37–44.

Dragan, E. S., & Apopei, D. F. (2011). Synthesis and swelling behavior of pH-sensitive semi-interpenetrating polymer network composite hydrogels based on native and modified potatoes starch as potential sorbent for cationic dyes. *Chemical Engineering Journal*, *178*, 252–263.

Dragan, E. S., Cazacu, M., & Nistor, A. (2009). Ionic organic/inorganic materials. III. Stimuli responsive hybrid hydrogels based on oligo(N,N-dimethylaminoethylmethacrylate) and chloroalkyl-functionalized siloxanes. *Journal of Polymer Science Part A: Polymer Chemistry*, *47*, 6801–6813.

Dragan, E. S., Perju, M. M., & Dinu, M. V. (2012). Preparation and characterization of IPN composite hydrogels based on polyacrylamide and chitosan and their interaction with ionic dyes. *Carbohydrate Polymers*, *88*, 270–281.

Hajizadeh, S., Kirsebom, H., Galaev, I. Y., & Mattiasson, B. (2010). Evaluation of selective composite cryogel for bromate removal from drinking water. *Journal of Separation Science*, *33*, 1752–1759.

Ilavsky, M., Hrouz, J., Stejskal, J., & Bouchal, K. (1984). Phase transition in swollen gels. 6. Effect of aging on the extent of hydrolysis of aqueous polyacrylamide solutions and on the collapse of gels. *Macromolecules*, *17*, 2868–2874.

Jain, E., Karande, A. A., & Kumar, A. (2011). Supermacroporous polymer-based cryogel bioreactor for monoclonal antibody production in continuous culture using hybridoma cells. *Biotechnology Progress*, *27*, 170–180.

Jeon, Y. S., Lei, J., & Kim, J. H. (2008). Dye adsorption characteristics of alginate/polyaspartate hydrogels. *Journal of Industrial and Engineering Chemistry*, *14*, 726–731.

Kang, H.-W., Tabata, Y., & Ikada, Y. (1999). Fabrication of porous gelatin scaffolds for tissue engineering. *Biomaterials*, *20*, 1339–1344.

Karmakar, N. C., Rath, S. K., Sastry, B. S., & Singh, R. P. (1998). Investigation on flocculation characteristics of polysaccharide-based graft copolymers in coal fines suspension. *Journal of Applied Polymer Science*, *70*, 2619–2625.

Kathuria, N., Tripathi, A., Kar, K. K., & Kumar, A. (2009). Synthesis and characterization of elastic and macroporous chitosan–gelatin cryogels for tissue engineering. *Acta Biomaterialia*, *5*, 406–418.

Kim, B., La Flamme, K., & Peppas, N. A. (2003). Dynamic swelling behavior of pH-sensitive anionic hydrogels used for protein delivery. *Journal of Applied Polymer Science*, *89*, 1606–1613.

Kim, D., & Park, K. (2004). Swelling and mechanical properties of superporous hydrogels of poly(acrylamide-co-acrylic acid)/polyethylenimine interpenetrating polymer networks. *Polymer*, *45*, 189–196.

Kim, B., & Shin, Y. (2007). pH-sensitive swelling and release behaviors of anionic hydrogels for intelligent drug delivery system. *Journal of Applied Polymer Science*, *105*, 3656–3661.

Kirsebom, H., Topggard, D., Galaev, I., & Yu Mattiasson, B. (2010). Modulating the porosity of cryogels by influencing the nonfrozen liquid phase through the addition of inert solutes. *Langmuir*, *26*, 16129–16133.

Li, W., Zhao, H., Teasdale, P. R., John, R., & Zhang, S. (2002). Synthesis and characterisation of a polyacrylamide–polyacrylic acid copolymer hydrogel for environmental analysis of Cu and Cd. *Reactive and Functional Polymers*, *52*, 31–41.

Liang, S., Liu, L., Huang, Q., & Yam, K. L. (2009). Preparation of single or double-network chitosan/poly(vinyl alcohol) gel films through selectively cross-linking method. *Carbohydrate Polymers*, *77*, 718–724.

Liu, M., Liu, H., Bai, L., Liu, Y., Cheng, J., & Yang, G. (2011). Temperature swing adsorption of melamine on thermosensitive poly(N-isopropylacrylamide) cryogels. *Journal of Materials Science*, *46*, 4820–4825.

Lozinsky, V. L., Plieva, F. M., Galaev, I. Y., & Mattiasson, B. (2001). The potential of polymeric cryogels in bioseparation. *Bioseparation*, *10*, 163–188.

Murali Mohan, Y., Joseph, D. K., & Geckeler, K. E. (2007). Poly(N-isopropylacrylamide-co-sodium acrylate) hydrogels: Interactions with surfactants. *Journal of Applied Polymer Science*, *103*, 3423–3430.

Murthy, P. S. K., Mohan, Y. M., Sreeramulu, J., & Raju, K. M. (2006). Semi-IPNs of starch and poly(acrylamide-co-sodium methacrylate): Preparation, swelling and diffusion characteristics evaluation. *Reactive and Functional Polymers*, *66*, 1482–1493.

Orakdogen, N., Karacan, P., & Okay, O. (2011). Macroporous responsive DNA cryogel beads. *Reactive and Functional Polymers*, *71*, 782–790.

Ozmen, M. M., Dinu, M. V., Dragan, E. S., & Okay, O. (2007). Preparation of macroporous acrylamide-based hydrogels: Cryogelation under isothermal conditions. *Journal of Macromolecular Science Part A: Pure and Applied Chemistry*, *44*, 1195–1202.

Pradny, M., Lesny, P., Fiala, J., Vacik, J., Sloui, M., Michalek, J., et al. (2003). Macroporous hydrogels based on 2-hydroxyethyl methacrylate. Part 1. Copolymers of 2-hydroxyethyl methacrylate with methacrylic acid. *Collection of Czechoslovak Chemical Communications*, *68*, 812–822.

Reis, A. V., Guilherme, M. R., Moia, T. A., Mattoso, L. H. C., Muniz, E. C., & Tambourgi, E. B. J. (2008). Synthesis and characterization of a starch-modified hydrogel as potential carrier for drug delivery system. *Journal of Polymer Science Part A: Polymer Chemistry*, *46*, 2567–2574.

Qudsieh, Y., Fakhru' l-Razi, A., Kabbashi, N. A., Mirghani, M. E. S., Fandi, K. G., Alam, M. Z., et al. (2008). Preparation and characterization of a new coagulant based on the sago starch biopolymer and its application in water turbidity removal. *Journal of Applied Polymer Science*, *109*, 3140–3147.

Savina, I. N., Cnudde, V., D'Hollander, S., Van Hoorebeke, L., Mattiasson, B., Galaev, I. Y., et al. (2007). Cryogels from poly(2-hydroxyethyl methacrylate): Macroporous, interconnected materials with potential as cell scaffolds. *Soft Matter*, *3*, 1176–1184.

Savina, I. N., Gun'ko, V. M., Turov, V. V., Dainiak, M., Phillips, G. J., Galaev, I. Y., et al. (2011). Porous structure and water state in cross-linked polymer and protein cryo-hydrogels. *Soft Matter*, *7*, 4276–4283.

Savina, I. N., Mattiasson, B., & Galaev, I. Y. (2005). Graft polymerization of acrylic acid onto macroporous polyacrylamide gel (cryogel) initiated by potassium diperiodatocuprate. *Polymer*, *46*, 9596–9603.

Serizawa, T., Wakita, K., Kaneko, T., & Akashi, M. (2002). Thermoresponsive properties of porous poly(N-isopropylacrylamide) hydrogels prepared in the presence of nanosized silica particles and subsequent acid treatment. *Journal of Polymer Science Part A: Polymer Chemistry*, *40*, 4228–4235.

Tekin, K., Uzun, L., Şahin, C. A., Bektaş, S., & Denizli, A. (2011). Preparation and characterization of composite cryogels containing imidazole group and use in heavy metal removal. *Reactive and Functional Polymers*, *71*, 985–993.

Van Vlierberghe, S., Dubruel, P., & Schacht, E. (2011). Biopolymer-based hydrogels as scaffolds for tissue engineering applications: A review. *Biomacromolecules*, *12*, 1387–1408.

Wu, X. S., Hoffman, A. S., & Yager, P. (1992). Synthesis and characterization of thermally reversible macroporous poly(N-isopropylacrylamide) hydrogels. *Journal of Polymer Science Part A: Polymer Chemistry*, *30*, 2121–2129.

Zhang, X.-Z., Yang, Y.-Y., Chung, T.-S., & Ma, K.-X. (2001). Preparation and characterization of fast response macroporous poly(N-isopropylacrylamide) hydrogels. *Langmuir*, *17*, 6094–6099.

Zhao, Q., Sun, J., Ling, Q., & Zhou, Q. (2009). Synthesis of macroporous thermosensitive hydrogels: A novel method of controlling pore size. *Langmuir*, *25*, 3249–3254.

Zhao, Q., Sun, J., Lin, Y., & Zhou, Q. (2010). Study of the properties of hydrolyzed polyacrylamide hydrogels with various pore structures and rapid pH-sensitivities. *Reactive and Functional Polymers*, *70*, 602–609.

Zhao, Q., Sun, J., Wu, X., & Lin, Y. (2011). Macroporous double-network cryogels: Formation mechanism, enhanced mechanical strength and temperature/pH dual sensitivity. *Soft Matter*, *7*, 4284–4293.